Molecular Microbiology (2004) **54**(3), 808–822 doi:10.1111/j.1365-2958.2004.04316.x

Integration host factor is involved in transcriptional regulation of the *Brucella abortus virB* operon

Rodrigo Sieira,[1] Diego J. Comerci,[1,2] Lía I. Pietrasanta[3] and Rodolfo A. Ugalde[1]*

[1]*Instituto de Investigaciones Biotecnológicas, Universidad Nacional de General San Martín, CONICET, San Martín 1650, Buenos Aires, Argentina.*

[2]*Comisión Nacional de Energía Atómica, División Agropecuaria, Centro Atómico Ezeiza 1804, Buenos Aires, Argentina.*

[3]*Centro de Microscopías Avanzadas, Facultad de Ciencias Exactas y Naturales, Universidad de Buenos Aires, Ciudad Universitaria, Pabellón I 1428, Buenos Aires, Argentina.*

Summary

Type IV secretion systems (T4SSs) are multicomponent machineries that play an essential role in pathogenicity of many facultative intracellular bacteria. The *virB* operon of *Brucella abortus* codes for a T4SS essential for virulence and intracellular multiplication. Here, virB expression analyses carried out using *lacZ* transcriptional fusions showed that *virB* promoter (P_{virB}) is temporally activated within J774 cells. Primer extension experiments revealed that virB transcription starts at 27 bp upstream of the first gene of the *virB* operon. Structural analyses showed that P_{virB} and regulatory sequences involved in intracellular regulation span 430 bp upstream of the transcription start site. A protein able to bind P_{virB} was isolated and identified. This protein, homologue to integration host factor (IHF), specifically interacts with P_{virB} and induces a DNA bending with an angle of 50.36°. DNAse I footprinting experiments showed that IHF protects a 51 bp region that contains two overlapped IHF binding consensus motifs. VirB expression experiments carried out with P_{virB}-*lacZ* fusions showed that in *B. abortus* IHF participates in the regulation of P_{virB} activity during the intracellular and vegetative growth in different media. A mutant strain with a 20 bp IHF binding site replacement failed to turn on the *virB* operon during the initial stages of macrophage infection and displayed severe intracellular multiplication defects. These data indicate that IHF plays a key role during intracellular *virB* operon expression being required for the biogenesis of the endoplasmic reticulum-derived replicative vacuole.

Accepted 19 July, 2004. *For correspondence. E-mail rugalde@iib.unsam.edu.ar; Tel. (+54) 11 4580 7255; Fax (+54) 11 4752 9639.

Introduction

Brucella spp. are Gram-negative facultative intracellular pathogens that belong to the alpha-2 subgroup of *Proteobacteria*. Several genera of this group, such as *Agrobacterium*, *Rickettsia* and *Rhizobium*, establish close relationships with eukaryotic organisms as pathogens or as endosymbionts. *Brucella* spp. infect many domestic mammals causing brucellosis, a chronic infectious disease that produces abortion in pregnant females and sterility in males (Corbel, 1997). Three species of the genus, *Brucella abortus*, *Brucella melitensis* and *Brucella suis* (whose preferred hosts are cattle, goats and pigs, respectively), are also able to produce zoonotic infections in humans. The clinical manifestations of human brucellosis are undulant fever, endocarditis, osteoarticular complications and neurological disorders, producing serious consequences in chronic cases.

An essential trait of *Brucella* virulence resides in its ability to survive and replicate within infected cells. During this process, the bacterium is internalized in a vacuole and redirects its intracellular traffic in such a way that it avoids degradation by the endocytic pathway (Pizarro-Cerda *et al*., 1998). Subsequent interaction events with endoplasmic reticulum (ER) membranes allow the maturation of the *Brucella*-containing vacuole (bcv) into an intracellular replication compartment where the bacterium multiplies (Celli *et al*., 2003).

Recently, a type IV secretion system (T4SS) coded by an operon highly homologous to the *virB* locus of the related species *Agrobacterium tumefaciens* has been found in *Brucella* (O'Callaghan *et al*., 1999; Ugalde, 1999; Sieira *et al*., 2000). T4SSs are multicomponent secretion machineries that have evolved giving rise to systems with different functions. For example, in the plant pathogen *A. tumefaciens* the *virB* system mediates the secretion of the nucleoprotein T complex to the plant cell (Stachel and Nester, 1986; Thompson *et al*., 1988). The *tra* system of *Escherichia coli* and the *trb* system of *A. tumefaciens* are involved in conjugative

DNA transfer (Winans and Walker, 1985; Li *et al*., 1998). Many other pathogenic bacteria interact with their hosts making use of T4SSs as export machineries of effector proteins. This is the case for the *cag* system of *Helilcobacter pylori* (Covacci *et al*., 1999), the *ptl* system of *Bordetella pertussis* (Weiss *et al*., 1993) and the *dot/icm* system of *Legionella pneumophila* (Conover *et al*., 2003).

Studies from many laboratories showed that *virB* T4SS is the major determinant of *Brucella* virulence in mice (Hong *et al*., 2000; Lestrate *et al*., 2000; Sieira *et al*., 2000). *Brucella virB* mutants are unable to replicate, in both professional and non-professional phagocytes (O'Callaghan *et al*., 1999; Sieira *et al*., 2000). It was also demonstrated that *virB* genes play an essential role in the maturation of the bcv into an intracellular replication niche (Comerci *et al*., 2001; Celli *et al*., 2003).

We have described that when *B. abortus* is grown in rich medium the *virB* operon is transcriptionally activated at the beginning of the stationary phase of growth (Sieira *et al*., 2000). The same behaviour was observed in *Brucella ovis*, *Brucella canis* and *B. melitensis* (Rouot *et al*., 2003). However, in *B. suis* the *virB* operon is inactive when grown in rich medium, requiring minimal medium and acidic pH for optimal activation (Boschiroli *et al*., 2002; Rouot *et al*., 2003). These findings indicate that *virB* regulation differs among *Brucella* species. Studies carried out with *B. melitensis* allowed the identification of an acyl-homoserine lactone in spent culture supernatants. The addition of a synthetic acyl-homoserine lactone reduced *virB* transcription in *B. suis* and *B. melitensis*, suggesting that a quorum-sensing system could be involved in the regulation of *Brucella virB* operon inside the host cell (Taminiau *et al*., 2002). Intracellular regulation studies of *B. suis virB* operon showed that the *virB* promoter (P_{virB}) is induced in J774 macrophages within 3 h post infection (p.i.), and that phagosome acidification is one of the signals that induce its expression (Boschiroli *et al*., 2002).

In the present work, we focused on the study of the regulation of *B. abortus* P_{virB}. We show a detailed analysis of intracellular virB expression in J774 cells. Analysis of P_{virB} structure revealed the transcription start site and regulatory sequences involved in intracellular activity. An homologue of integration host factor (IHF), a protein known to be involved in transcriptional regulation of a wide variety of bacterial genes, was isolated and identified by tandem mass spectrometry. Specificity of binding to P_{virB}, affinity and binding site of IHF were analysed. We also demonstrated that in *B. abortus* IHF is able to induce a DNA bending and plays a relevant role in regulation of P_{virB} activity either during intracellular or during vegetative growth in different media.

Results

Brucella abortus virB *expression during vegetative growth*

In order to study the regulation of *B. abortus* 2308 P_{virB}, a 453 bp DNA fragment located upstream *virB1* gene was transcriptionally fused to *lacZ* and cloned into a suicide vector that does not replicate in *Brucella*. This construct was used to generate strain *B. abortus* P_{virB}::*lacZ*, which contains a single P_{virB}::*lacZ* transcriptional fusion and a copy of P_{virB} that controls the *virB* operon expression. This strain was used to determine β-galactosidase activity during the growth curve in rich medium. Figure 1A shows that during the initial stages of growth strain *B. abortus* P_{virB}::*lacZ* displayed low levels of β-galactosidase activity. After 20 h of growth, three- to four-fold activation was observed. These results indicate that construct P_{virB}::*lacZ* is transcriptionally activated in rich medium with a pattern similar to that previously observed with a chromosomal *lacZ* transcriptional fusion to *virB10* (Sieira *et al*., 2000).

VirB7 expression was analysed by Western blot using a rabbit anti-serum prepared against a *B. abortus* histidine-tagged VirB7 recombinant protein. Cell lysates from *B. abortus* 2308 wild type and from a *virB1* polar mutant strain were obtained from cultures harvested during the exponential or the stationary phase of growth. As shown in Fig. 1B, VirB7 expression was detected only in stationary phase lysates of the wild-type strain. These results indicate that the DNA region fused to the reporter gene behaves as the native promoter, thus validating the use of this P_{virB}::*lacZ* fusion in the studies described below.

Intracellular B. abortus virB *expression*

Recently, Boschiroli *et al*. (2002) showed that the *B. suis virB* operon is induced in macrophages within 3 h p.i. To determine whether *B. abortus* virB expression is regulated within the host cell, intracellular P_{virB} activity was examined after infecting J774 macrophages with the strain *B. abortus* P_{virB}::*lacZ*. In order to start infection with the reporter system in a non-activated state, macrophage infection experiments were carried out with bacteria obtained from cultures harvested during the exponential phase of growth. Thirty minutes after infection, a mix of antibiotics was added to the medium to eliminate remaining extracellular bacteria. At different p.i. times, β-galactosidase activity per viable intracellular bacterium was determined as described in *Experimental procedures*. As shown in Fig. 1C, intracellular *virB* transcription was induced after internalization, reaching maximal activation at 5 h p.i. Afterwards, β-galactosidase activity decreased reaching similar levels to that observed at the beginning of the infection. These results show that *virB* transcription is tightly regulated during the infection process, being active

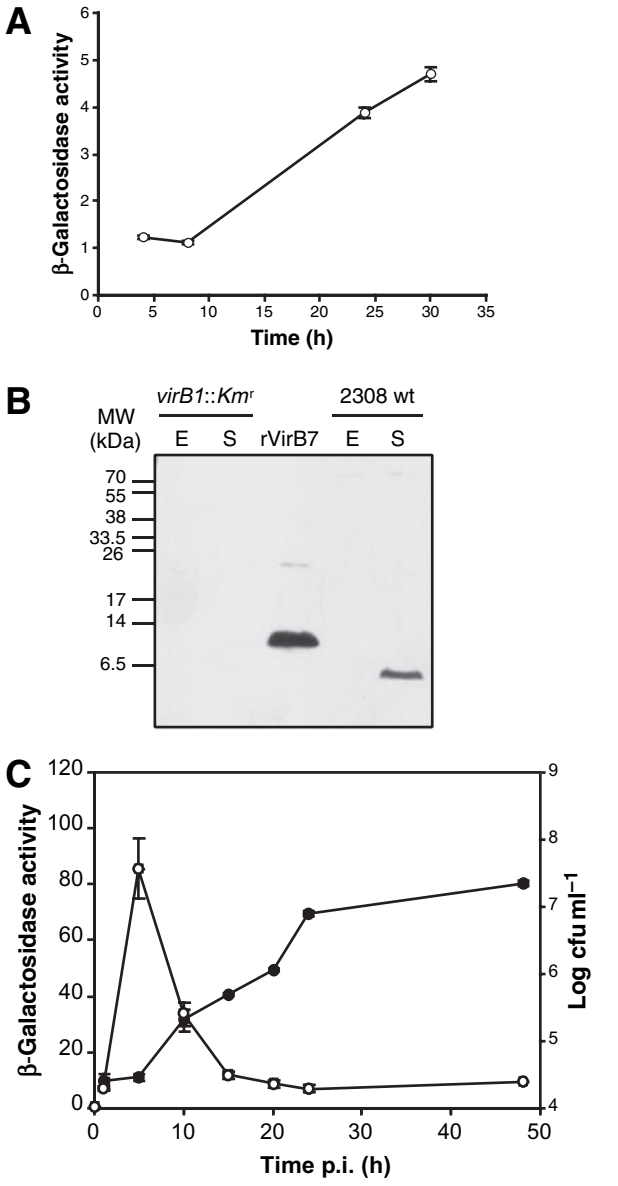

Fig. 1. Analysis of virB expression under different growth conditions.
A. Expression of chromosomal P_{virB}::*lacZ* transcriptional in wild-type strain *B. abortus* 2308. Cultures of strain *B. abortus* P_{virB}::*lacZ* were grown overnight in rich medium (TSB), diluted 1:50 in fresh medium and assayed for β-galactosidase activity at different times. Values are means ± standard deviations of duplicate samples from a representative of three independent experiments.
B. Western blot analysis. Wild-type *B. abortus* 2308 or *virB1*::Km^r mutant strains were grown in TSB and harvested during exponential (E) or stationary (S) phase of growth. Samples corresponding to equal numbers of bacteria or recombinant VirB7 protein (rVirB7) were submitted to 15% tricine-PAGE, transferred to nitrocellulose membranes and developed with anti-VirB7 polyclonal anti-serum. Position of molecular weight markers is indicated.
C. Intracellular virB expression in J774 macrophages. J774 cells were infected with strain *B. abortus* P_{virB}::*lacZ*. At the indicated times, cells were disrupted, centrifuged and β-galactosidase activity (open circles) and cfu ml^{-1} (solid circles) were determined. Values are means ± standard deviations of triplicate wells from a representative of three independent experiments.

during the initial stages of infection and turned off before intracellular bacteria start replicating.

Structure of B. abortus virB *promoter*

The P_{virB} transcription start site was identified by primer extension experiments using total RNA extracted from *B. abortus* 2308 stationary phase cultures. As shown in Fig. 2A, a single band was detected, indicating that *virB* transcription starts at a unique site located 27 bp upstream the start codon of *virB1* gene (Fig. 2B).

In order to identify the minimal region necessary for promoter activity, P_{virB} fragments of different length were fused to *lacZ* and cloned into the intermedium copy-number plasmid pBBR1MCS-4 (schematized in Fig. 3A). *Brucella* strains containing different constructs were analysed for β-galactosidase activity during vegetative and intracellular growth. Figure 3B shows that *B. abortus* 2308 transformed with plasmid p5, which contains a 453 bp DNA fragment located upstream *virB1* gene, or with the control plasmid p0 with no insert, have similar β-galactosidase activity during the initial stages of growth. However, after 20 h of growth, two- to threefold activation was observed only with the strain carrying plasmid p5, thus indicating that this DNA region contains promoter activity with the same activation pattern as that observed with the

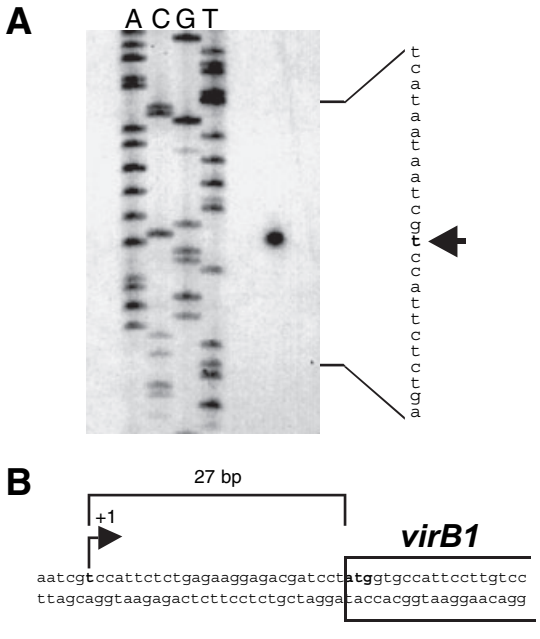

Fig. 2. Structure of *B. abortus* P_{virB}.
A. Primer extension analysis was performed using total RNA from stationary-phase cultures of *B. abortus* 2308 grown in TSB and the radiolabelled primer pvirdown II. The arrow indicates the transcription start site. Lanes A, C, G and T show the sequencing reaction using the same primer. Right lane shows the primer extension product.
B. Sequence of *B. abortus virB* promoter region. Transcription start site (+1) and the 5′ end of *virB1* gene are indicated.

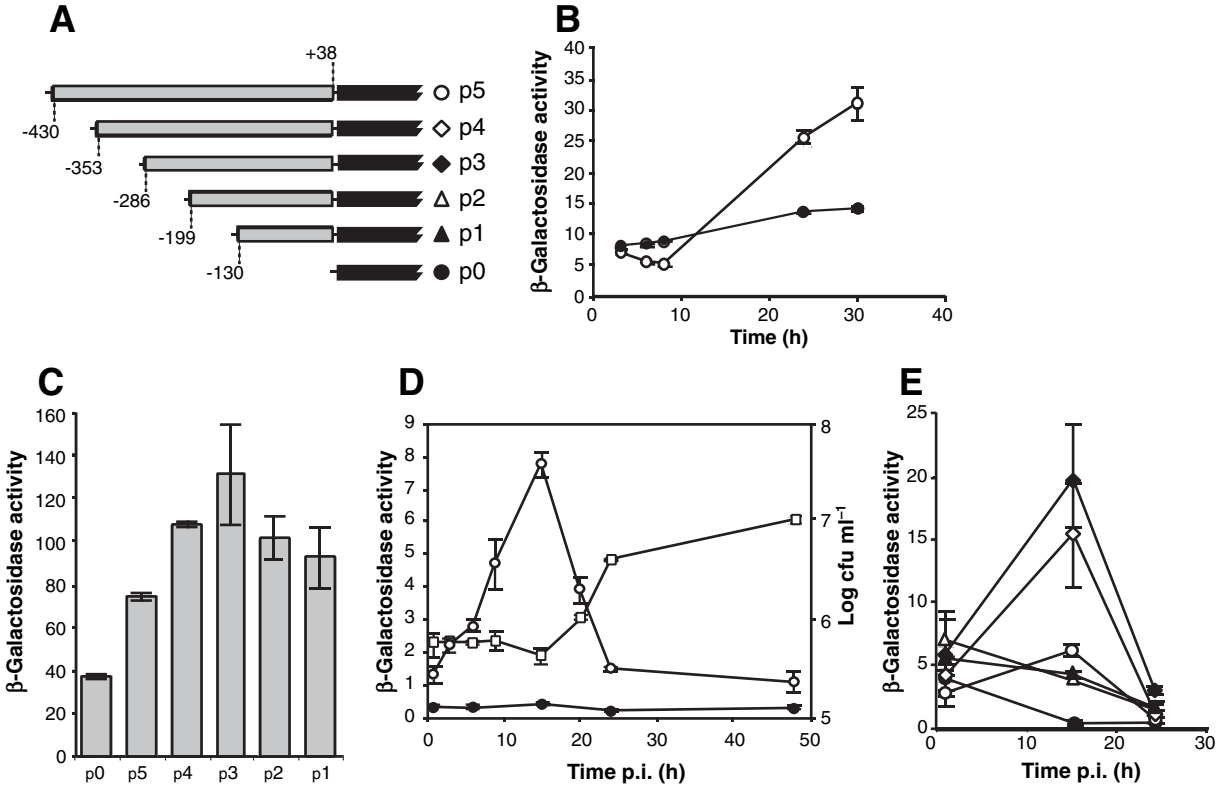

Fig. 3. Identification of the minimal region of P_{virB} necessary for intracellular activation.
A. Schematic representation of plasmid transcriptional fusions of P_{virB} fragments of different length to *lacZ*. Grey bars represent the different P_{virB} fragments. Positions relative to transcription start site are indicated for each construction. Black bars represent promoterless *lacZ* cassette.
B. Expression of plasmid P_{virB}::*lacZ* transcriptional fusion (p5) (open circles) and control plasmid with no insert (p0) (solid circles) in wild-type strain *B. abortus* 2308. Cultures were grown overnight in TSB, diluted 1:50 in fresh medium and assayed for β-galactosidase activity at different times. Values are means ± standard deviations of duplicate samples from a representative of three independent experiments.
C. Expression of different P_{virB} fragments during vegetative growth. Overnight cultures of *B. abortus* 2308 strains carrying constructions schematized in (A) grown in TSB were diluted 1:50 in fresh medium and assayed for β-galactosidase activity in stationary phase (OD_{600} = 3–3.5). Values are means ± standard deviations of duplicate samples from a representative of three independent experiments.
D. Intracellular expression of plasmid P_{virB}::*lacZ* transcriptional fusion in J774 macrophages. J774 cells were infected with *B. abortus* 2308 carrying P_{virB}::*lacZ* transcriptional fusion (open circles) or control plasmid with no insert (solid circles). At the indicated times, cells were disrupted, centrifuged and β-galactosidase activity was determined. cfu ml^{-1} of the strain carrying P_{virB}::*lacZ* transcriptional fusion was determined (open squares). Values are means ± standard deviations of triplicate wells from a representative of three independent experiments.
E. Intracellular expression of different P_{virB} fragments in J774 macrophages. J774 cells were infected with *B. abortus* 2308 strains carrying constructions schematized in (A). β-Galactosidase activity was determined as described in Fig. 1C. Values are means ± standard deviations of duplicate wells from a representative of three independent experiments.

chromosomal P_{vir}::*lacZ* trascriptional fusion shown in Fig. 1A. β-Galactosidase activity displayed by the different P_{virB} fragments (schematized in Fig. 3A) was determined in stationary phase cultures in tryptic soy broth (TSB) medium. As shown in Fig. 3C, all the constructs, except plasmid p0, displayed higher promoter activity than plasmid p5. These results suggest that during vegetative growth the DNA region spanning position −130 to +1 is sufficient to support promoter activation and that the region spanning position −430 to −353 is involved in promoter downregulation.

The intracellular P_{virB} activity of plasmid p5 was analysed in J774 cells. As shown in Fig. 3D, intracellular *virB* transcription was induced after internalization, reaching a maximal of 20- to 30-fold activation at 15 h p.i. Afterwards, β-galactosidase activity decreased reaching similar levels to that observed at the beginning of the infection. On the other hand, the control plasmid p0 did not show any variation of β-galactosidase activity during the experiment. This behaviour is similar to that observed with the chromosomal transcriptional fusion described in Fig. 1C. However, the time of maximal activation of plasmid p5 (15 h p.i.) was delayed compared with that of the chromosomal construct (5 h p.i.), probably due to the effect produced by the plasmid multicopy. In view of these results, the intracellular β-galactosidase activity of strains carrying different P_{virB}::*lacZ* fusions was measured in J774 cells at 1, 15 and 24 h p.i. As shown in Fig. 3E, plasmids p0, p1 and p2 did not show intracellular activation at 15 h. On the other hand, plasmids p3, p4 displayed as p5 maximal activity at

15 h p.i. and were turned off at 24 h p.i. However, β-galactosidase activity of these constructs was three- to fourfold higher than p5, suggesting that the region spanning positions –353 to –430 plays a role in the intracellular P_{vir} regulation attenuating VirB expression as it was observed during vegetative growth.

Unlike what observed during vegetative growth, in the intracellular environment only those DNA regions containing at least 286 bp upstream the transcription start site were transcriptionally activated. These findings suggest that within the host cell the *B. abortus* P_{virB} is under the control of complex regulation mechanism(s) different from those acting during the vegetative growth.

Identification of virB *transcription factors*

To identify putative transcriptional regulators of *virB* operon, we analysed by gel shift assays the presence of DNA-binding proteins in crude extracts of *B. abortus* 2308. A radiolabelled DNA fragment spanning positions –201 to +24 relative to the transcription start site was used as probe. As shown in Fig. 4A, retarded bands were observed when the probe was incubated with either exponential or stationary phase cell extracts. To analyse specificity and localization of the observed protein–DNA complex (complex I), gel shift assays were carried out using different P_{virB} fragments as unlabelled competitors (schematized in Fig. 4B). Figure 4C shows that the retarded band was only competed with the full-length probe or with fragment C1, thus indicating that the observed protein–DNA interaction is localized between positions –201 and –130. Incubation of crude cell extracts with specific or non-specific radiolabelled DNA probes also showed that binding is specific and is localized in the above-mentioned position (data not shown). These results suggested that a putative *virB* transcription factor is present in *B. abortus* during vegetative growth in rich medium both in exponential and stationary phase.

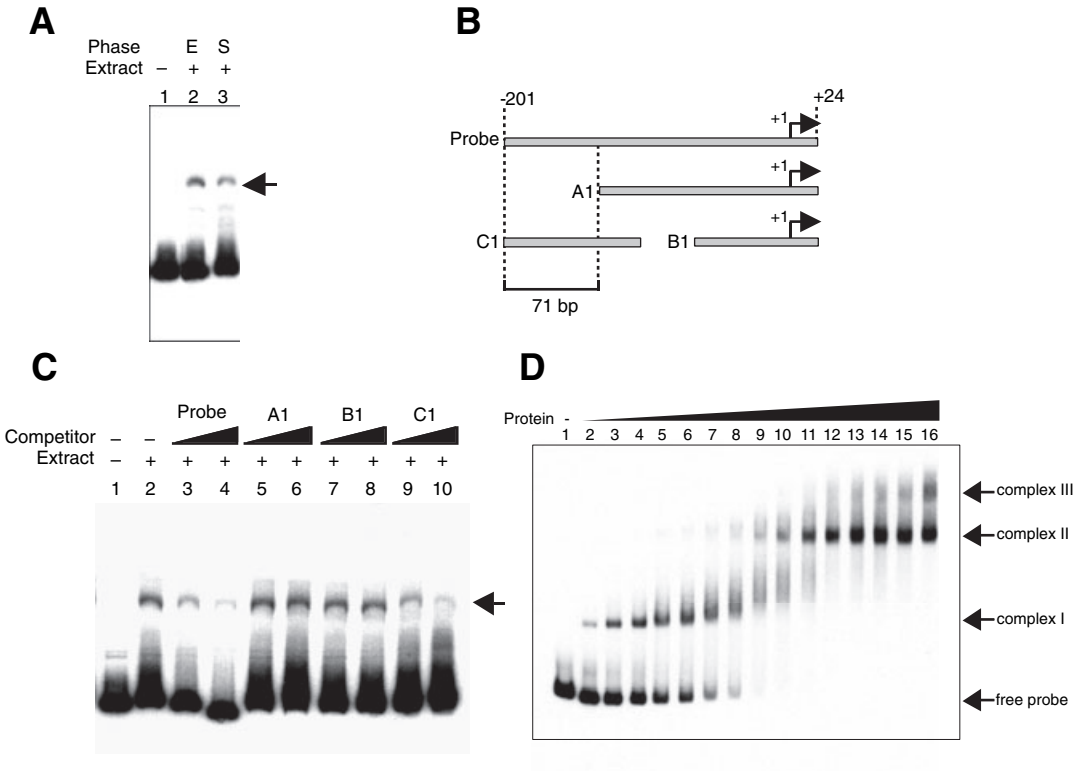

Fig. 4. Detection of DNA-binding activity to P_{virB} in extracts of *B. abortus* 2308.
A. Gel shift assay was performed using a radiolabelled P_{virB} fragment (–201 to +24) and *B. abortus* 2308 crude extracts from exponential (E, lane 2) or stationary (S, lane 3) phase cultures grown in TSB. Protein concentration of crude extracts in each reaction was as follows: lane 1, no protein; lanes 2 and 3, 7 μg. Complex I is indicated by an arrow.
B. Schematic representation of P_{virB} fragments used as unlabelled DNA competitors.
C. Gel shift competition assay using crude protein extracts obtained from stationary phase cultures and different unlabelled DNA fragments indicated in (B) as competitors. Protein concentration was as follows: lane 1, no protein; lanes 2–10, 7 μg. The concentration of unlabelled DNA competitors in each reaction was as follows: lanes 1 and 2, no competitor DNA; lanes 3, 5, 7 and 9, 100 ng; lanes 4, 6, 8 and 10, 360 ng.
D. Band shift pattern of partially purified extracts of *B. abortus* 2308. Gel shift assay was performed using a radiolabelled fragment of P_{virB} (–201 to +24) and increasing concentrations of a partially purified DEAE-eluted fraction. Protein concentration in each reaction was as follows: lane 1, no protein; lanes 2–16, 0.5–7.5 μg increasing 0.5 μg per lane). Positions of free probe and complexes I, II and III are indicated.

Based on these findings, a purification protocol was set up in order to isolate the DNA-binding protein(s) responsible for the formation of the observed complex. DNA-binding activity was followed during purification by gel shift assay using the probe –201 to +24 (see Fig. 4B). The band shift pattern of a partially purified extract obtained from DEAE chromatography was examined using increasing amounts of protein. Figure 4D shows that besides the previously observed complex I, two additional complexes were formed at high-protein concentrations. Further purification was achieved by affinity chromatography using a biotin-labelled –201 to +24 probe bound to streptavidin-coated paramagnetic spheres. Affinity chromatography was carried out under the same conditions used to perform gel shift assays, including non-specific competitor DNA. A single band with mobility corresponding to a mass of about 12 kDa was obtained. This protein was recovered from the gel and identified by tandem mass spectrometry. Two peptides (TGEEVPILPRR and LSSFATFQVR) that match with *B. melitensis* and *B. suis* IHF α-subunit (predicted molecular mass 11.9 kDa) were identified.

Characterization of the P_{virB}–IHF interaction

The identification of IHF as a putative P_{virB}-binding protein prompted us to clone and purify a recombinant *B. abortus* IHF (rIHF). The ability of rIHF to bind P_{virB} was analysed by gel shift assay using the probe –201 to +24. As shown in Fig. 5A, rIHF gave rise to complex I formation and two additional complexes at higher-protein concentrations. This pattern is indistinguishable to that observed with partial purified native extracts (see Fig. 4D).

To test the specificity of the binding between rIHF and P_{virB}, a gel shift experiment was carried out using specific and unspecific radiolabelled DNA probes, or different unlabelled DNA fragments as competitors. Figure 5B shows that rIHF did not bind to radiolabelled DNA containing a region of *B. abortus virB10*. After incubation of rIHF with a radiolabelled P_{virB} fragment, a retarded band corresponding to complex I was observed. Competition with increasing concentrations of an unlabelled fragment of P_{virB} completely displaced complex I formation, whereas competition with an unlabelled fragment of *B. abortus virB10* had no effect. These results demonstrate that rIHF binds to P_{virB} in a specific manner. Gel shift assays were carried out in duplicate using rIHF and the probe –201 to +24. The amount of free and protein-bound DNA was estimated by measuring the intensity of autoradiograms and the apparent dissociation constant (K_d) of the IHF–P_{virB} complex was calculated as described in *Experimental procedures.* The K_d of IHF for its P_{virB} binding site was estimated to be 185 nM (Fig. 5C).

In order to identify the IHF binding site, a DNaseI footprinting assay was performed using the same P_{virB} DNA fragment used in gel shift experiments. Figure 6A shows that rIHF protected a 51 bp DNA region that spans positions –188 to –137. Several DNaseI-hypersensitive sites located within the protected region were observed. Figure 6B shows the location of the protected

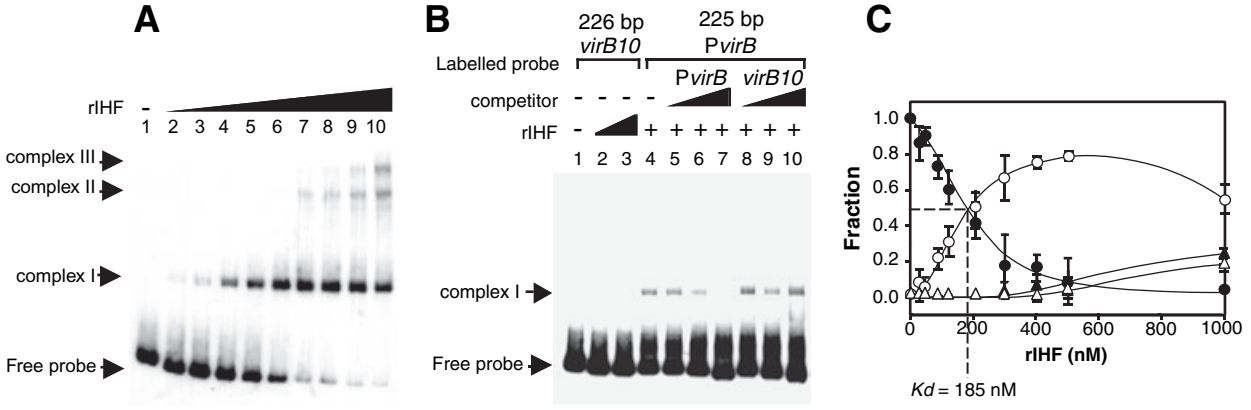

Fig. 5. DNA-binding activity of recombinant *B. abortus* IHF (rIHF).
A. Band shift pattern of rIHF. Gel shift assay was performed with increasing concentrations of rIHF and radiolabelled P_{virB} (fragment –201 to +24). rIHF concentration in each reaction was as follows: lane 1, no protein; lane 2, 20 nM; lane 3, 40 nM; lane 4, 80 nM; lane 5, 120 nM; lane 6, 200 nM; lane 7, 300 nM; lane 8, 400 nM; lane 9, 500 nM; lane 10, 1000 nM.
B. Specificity of rIHF binding to P_{virB}. Gel shift assay performed using rIHF and a 226 bp fragment of *B. abortus virB10* gene or the 225 bp P_{virB} fragment (–201 to +24) as radiolabelled probes or as unlabelled competitor DNAs. rIHF concentration in each reaction was as follows: lane 1, no protein; lane 2, 15 nM; lane 3, 30 nM; lanes 4–10, 20 nM. Mass of unlabelled competitor DNA in each reaction was as follows: lanes 1–4, no competitor DNA; lanes 5 and 8, 16 ng; lanes 6 and 9, 160 ng; lanes 7 and 10, 500 ng. Position of complex I is indicated by an arrow.
C. Formation of the complex rIHF–P_{virB}. Free and protein-bound DNA fractions of free probe (solid circles), complex I (open circles), complex II (solid triangles) or complex III (open triangles) were calculated by measuring the band intensity of the radioactive bands shown in (A). Values are means ± standard deviations of two independent measurements. The calculated apparent dissociation constant (K_d) is indicated.

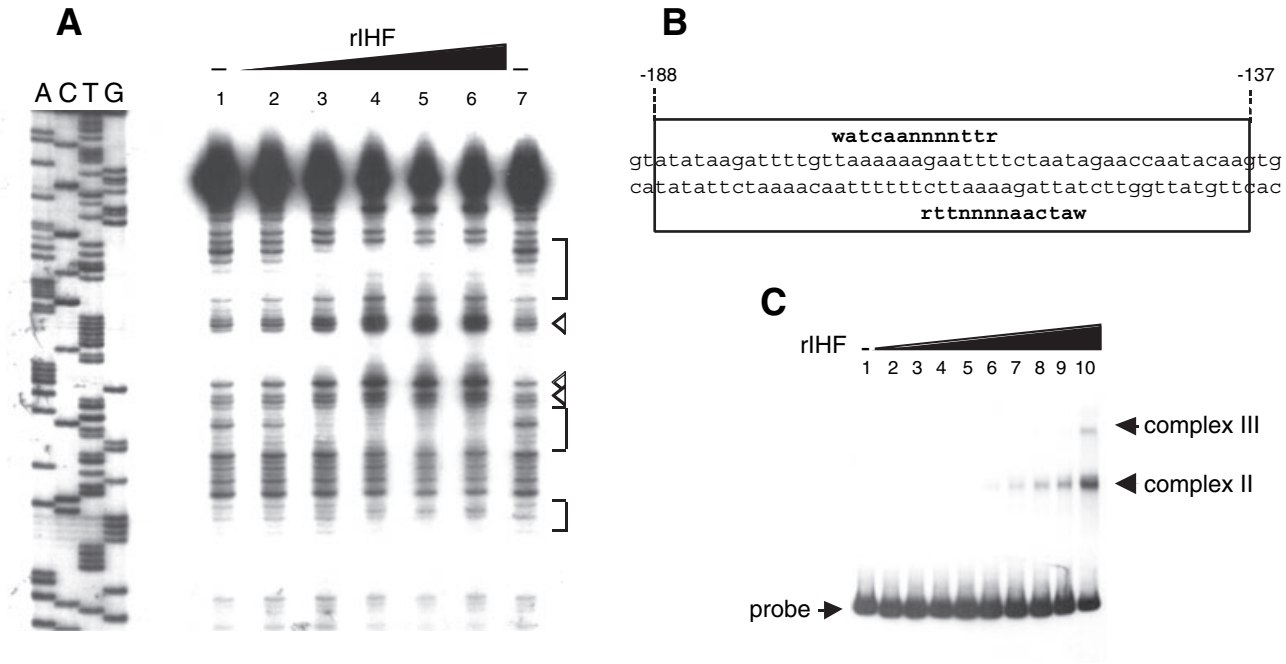

Fig. 6. Examination of rIHF binding site in P_{virB}.
A. DNase I footprinting analysis. A radiolabelled 225 bp P_{virB} fragment (–201 to +24) was incubated with different concentrations of rIHF and subjected to digestion with DNase I as described in *Experimental procedures*. The gel was calibrated with a DNA sequence reaction of the radiolabelled fragment (lanes A, C, T and G). rIHF concentration in each reaction was as follows: lanes 1 and 7, no protein; lane 2, 30 nM; lane 3, 120 nM; lane 4, 240 nM; lane 5, 360 nM; lane 6, 480 nM. Protected regions are indicated with brackets; DNase I-hypersensitive sites are indicated with open triangles.
B. Position of the protected region relative to P_{virB} transcription start site. DNAse I-protected region is indicated by an open box. *E. coli* consensus binding motifs for IHF is indicated in bold (W = A or T; N = any nucleotide; R = A or G).
C. Gel shift assay performed with rIHF and a P_{virB} fragment (–201 to +24) lacking the IHF binding site. rIHF concentration in each reaction was as follows: lane 1, no protein; lane 2, 20 nM; lane 3, 40 nM; lane 4, 80 nM; lane 5, 120 nM; lane 6, 200 nM; lane 7, 300 nM; lane 8, 400 nM; lane 9, 500 nM; lane 10, 1000 nM. Positions of free probe and complexes II and III are indicated.

region obtained by DNase I footprinting. Two sequences that partially match the *E. coli* IHF consensus binding motif WATCAANNNNTTR (where W = A or T; N = any nucleotide; and R = A or G) were identified within the DNAseI-protected region. These sequences are overlapped and located in the core of the DNase I-protected zone.

To determine whether the rIHF–P_{virB} binding results from a specific recognition of the consensus sequences, a gel shift experiment was performed using a probe that contains a replacement of the 20 bp putative IHF binding site by a non-related sequence ($P_{virB\text{-}IHF}$). As shown in Fig. 6C, the formation of complex I was totally abolished, whereas the formation of the other two complexes remained unaltered and appeared at the same rIHF concentrations as that observed with the wild-type probe (see Fig. 5A). These results indicate that IHF specifically recognizes a consensus motif located at the core of the DNase I-protected region and that the consensus sequence is similar to that of *E. coli*. The structure of the IHF–P_{virB} complex was analysed using atomic force microscopy (AFM), a technique that has the potential to assay protein–nucleic acid interactions for individual complexes at the molecular level (Bustamante and Rivetti, 1996; Pietrasanta *et al.*, 1999). A 512 bp DNA fragment, containing the IHF binding site near the centre of the DNA molecule, was incubated with rIHF and AFM images of rIHF–P_{virB} complexes were taken for analysis. Figure 7 shows that rIHF was bound near the centre of the DNA fragment, inducing an apparent DNA bending angle of 50.36° ± 26.67°. To determine whether the observed bend was an inherent characteristic of the P_{virB}-containing DNA fragment, representative molecules lacking complexes were examined for bending. The bend angle was determined at a position corresponding to the IHF binding site. Uncomplexed DNA molecules showed a bend angle distribution centred at 0° (data not shown), indicating that the DNA bending of the rIHF–P_{virB} complexes was induced by the binding of IHF. These observations represent a direct visualization of the rIHF–P_{virB} complex and demonstrate that binding of IHF modifies the promoter structure inducing a bending of DNA that probably participates in regulation of transcription.

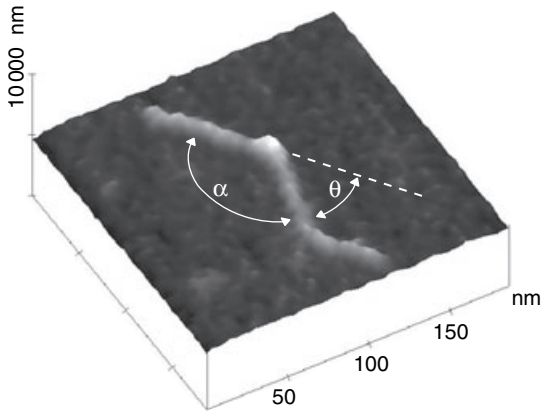

Fig. 7. IHF-dependent bending of P_{virB} DNA. AFM image of a rIHF–P_{virB} complex on mica showing the measured angle α and its relation to the bend angle θ ($\theta = 180 - \alpha$). The image is presented as surface plot at a 62° viewing angle to emphasize topography.

Role of IHF in regulation of the virB *promoter activity*

To assess the contribution of IHF on the activation of P_{virB}, we constructed a strain that harbours a single chromosomal transcriptional fusion with a 20 bp replacement of the IHF binding site consensus. It also contains a copy of the wild-type P_{virB} that controls *virB* operon expression (Fig. 8A). This strain (*B. abortus* $P_{virB\text{-}IHF}$::*lacZ*) was used to study the activity pattern during vegetative growth in rich medium (TSB), and minimal medium at pH 7.0 or 4.5.

Figure 8B shows that in TSB medium P_{virB} was upregulated during the stationary phase of growth as we have described above, whereas $P_{virB\text{-}IHF}$ was not activated in stationary phase and displayed the same β-galactosidase activity as in the exponential phase of growth. These results suggest that the mechanism by which P_{virB} is activated in stationary phase in rich medium is IHF dependent.

When bacteria were incubated in minimal medium at pH 7.0, it was observed that β-galactosidase activity of *B. abortus* P_{virB}::*lacZ* rapidly increased after 6 h of cultivation remaining active for 24 h (Fig. 8C) whereas β-galactosidase activity of $P_{virB\text{-}IHF}$::*lacZ* slowly increased during the experiment. This indicates that in minimal medium at pH 7.0 IHF is also involved in regulation of P_{virB} activity. In minimal medium at pH 4.5, however, IHF seems not to be directly involved in P_{virB} activation observed because *B. abortus* $P_{virB\text{-}IHF}$::*lacZ* displayed a similar activation pattern as the control strain under this culture condition (Fig. 8D).

The role of IHF in intracellular *virB* expression was studied in J774 cells using strains *B. abortus* P_{virB}::*lacZ* or *B. abortus* $P_{virB\text{-}IHF}$::*lacZ*. Figure 8E shows that *B. abortus* $P_{virB\text{-}IHF}$ exhibited a misregulated activity pattern compared with that of control strain, being unable to undergo the

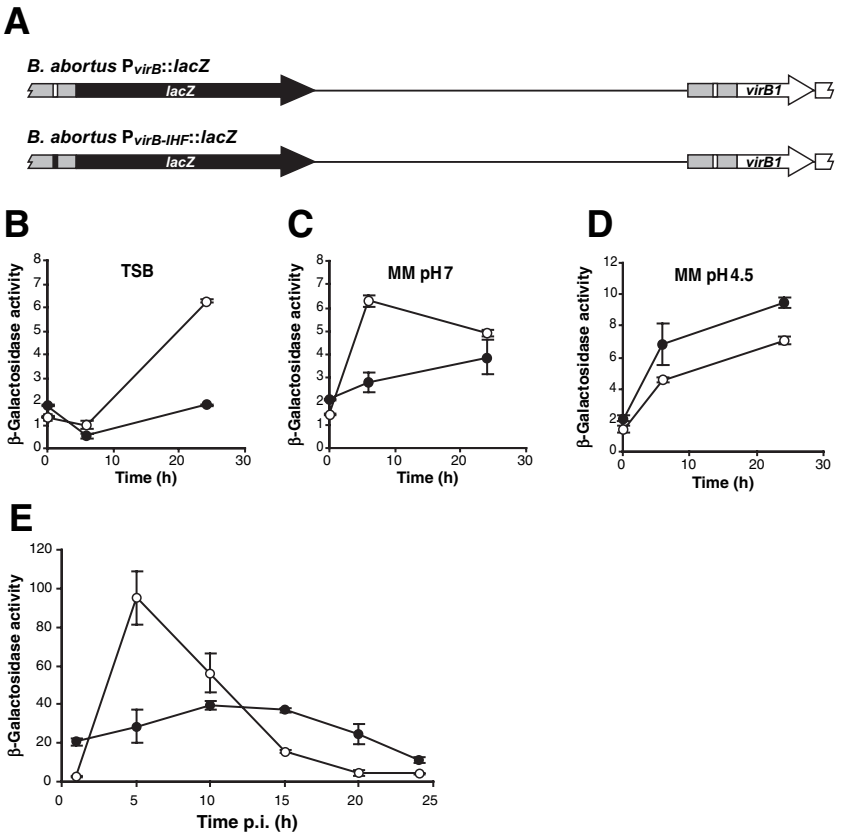

Fig. 8. Role of IHF on virB expression.
A. Schematic representation of chromosomal sequences of strains *B. abortus* P_{virB}::*lacZ* and *B. abortus* $P_{virB\text{-}IHF}$::*lacZ*. Grey bars represent sequences corresponding to P_{virB}. White boxes: wild-type IHF binding site. Black box: replacement of the IHF binding site. Black bars: promoterless *lacZ* cassette. White bars: sequences corresponding to the wild-type *virB* operon. Solid line: sequences corresponding to the suicide vector used for the construction of strains.
B–D. virB expression during vegetative growth in TSB (B), minimal medium (MM) at pH 7.0 (C) or MM at pH 4.5 (D). β-Galactosidase activity of strains *B. abortus* P_{virB}::*lacZ* (open circles) or *B. abortus* $P_{virB\text{-}IHF}$::*lacZ* (solid circles) was determined as follows: cultures grown until exponential phase (OD_{600} = 0.5–1) in TSB were harvested, washed with PBS, resuspended in fresh medium and incubated at 37°C with agitation. β-Galactosidase activity was assayed at different times. Values are means ± standard deviations of duplicate samples from a representative of two independent experiments.
E. Intracellular virB expression. J774 cells were infected with strains *B. abortus* P_{virB}::*lacZ* or *B. abortus* $P_{virB\text{-}IHF}$::*lacZ*. Infection and β-galactosidase activity determinations were performed as described above.

characteristic activity peak during the initial stages of infection and the subsequent downregulation. These findings show that IHF plays a determinant role on P_{virB} regulation either in vegetative or in intracellular lifestyle.

Effect of IHF on intracellular multiplication of B. abortus *in J774 cells*

The misregulated pattern of VirB transcription exhibited by strain *B. abortus* $P_{virB\text{-}IHF}$ prompted us to assess the effect of IHF-mediated regulation of P_{virB} on *B. abortus* macrophage infection. Virulent *B. abortus* 2308 and its isogenic derivative *B. abortus* H1, which lacks the IHF binding site of P_{virB} due to a 20 bp replacement, were used to infect J774 macrophages and the number of intracellular bacteria was determined at different p.i. times. Whereas the parental virulent strain was able to sustain intracellular replication reaching 1.68×10^6 cfu at 24 h, the number of intracellular *B. abortus* H1 decreased exponentially during the first 24 h p.i. (Fig. 9). Afterwards, this mutant was able to replicate reaching 1.51×10^4 cfu ml^{-1} at 48 h. This indicates that IHF is essential for the proper activity of P_{virB} necessary for the crucial process of establishment of an ER-derived replicative organelle.

Discussion

In this work, we have analysed, by means of chromosomal *lacZ* transcriptional fusions, the expression of the *B. abortus virB* operon both under vegetative and intracellular growth conditions. Upon macrophage infection, the operon is rapidly turned on, remaining active during the time the bacterium is promoting the biogenesis of the replicative organelle. When the intracellular replicative compartment was established and the intracellular exponential replication starts, the operon is repressed. We have identified IHF as one of the transcription factors affecting *virB* expression. A mutant strain harbouring a P_{virB} IHF binding site replacement showed misregulation of *virB* operon and was unable to efficiently infect macrophages. Thus, activity of P_{virB} depends on the action of the nucleoid protein IHF, which affects transcription probably by providing the proper promoter structure for the action of other yet unknown transcriptional factors.

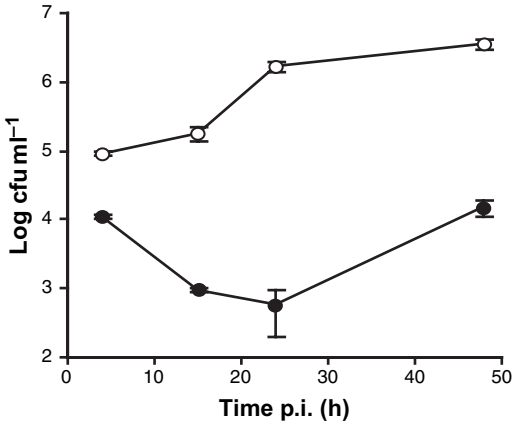

Fig. 9. Intracellular replication of parental *B. abortus* 2308 (open circles) and mutant *B. abortus* H1 (solid circles) strains in J774 macrophages. Values are means ± standard deviations of duplicate wells from a representative of two independent experiments.

We showed that P_{virB} is activated intracellularly at the initial stages of infection, reaching its maximal activity at 5 h p.i., afterwards the promoter is turned off (Fig. 1C). During this period, *Brucella* actively promotes interaction of the bcv with the ER, a key process for the biogenesis of the replicative compartment (Celli and Gorvel, 2004). The *virB* operon is active throughout this definite and narrow period of time; afterwards, it is downregulated. This downregulation seems to be a necessary condition before bacterial multiplication occurs. Previous works have showed that expression of the entire *virB* operon in an intermedium copy-number plasmid partially inhibited intracellular multiplication of *B. suis*. It was suggested that the VirB apparatus is needed during the initial stages of infection but its subsequent expression would be detrimental for the bacteria (O'Callaghan *et al*., 1999; Taminiau *et al*., 2002).

Brucella abortus virB expression during vegetative growth in rich medium was analysed by Western blot and β-galactosidase activity assays. The promoter is active during the stationary phase of growth in rich medium (Fig. 1A–B), which is consistent with results obtained by different methods (Sieira *et al*., 2000). However, when grown in minimal medium at either pH 7.0 or 4.5, VirB is active during the exponential phase of growth. A previous work had shown that *virB* regulation differs among *Brucella* species (Rouot *et al*., 2003). Unlike *B. abortus* and *B. melitensis*, the *B. suis virB* operon is only expressed in minimal medium at pH 4.5 but not in rich medium or minimal medium at pH 7.0. It is remarkable that DNA sequence comparison of the promoter region of the *virB* operon did not show any difference between the three species. Moreover, a detailed whole genome comparison among *B. abortus*, *B. suis* and *B. melitensis* showed that the main genetic differences between these species may result from gene inactivation, mainly of genes coding for transcriptional regulators and surface structures (D.J. Comerci, unpubl. data). These observations suggest that in *B. suis* P_{virB} could be under the control of regulation pathways that differ from those of *B. abortus* and *B. melitensis.*

In the present study, we identified a transcriptional regulator of *Brucella virB* operon. Two independent affinity purification experiments led to the isolation of the α-subunit of an IHF homologue. We showed that IHF is

necessary for the appropriate activation of P_{virB} both during vegetative growth and within the host cell. The analyses of transcriptional fusions lacking the IHF binding site showed that P_{vir} is controlled by IHF-dependent mechanisms at pH 7.0 in both rich and minimal medium. However, during growth under acidic conditions the promoter is activated after 6 h by IHF-independent mechanisms.

Intracellular replication experiments carried out with the mutant strain *B. abortus* H1 suggest that binding of IHF to a 20 bp sequence of the promoter is necessary for the proper control of the initial intracellular trafficking steps and to avoid degradation by the lysosomes. However, after 24 h of infection, although in small numbers, the mutant strain was recovered from the macrophages, thus suggesting that a small proportion of internalized bacteria avoided fusion with lysosomes reaching the intracellular replication niche. The phenotype of strain *B. abortus* H1 is clearly different from that of mutants on structural genes such as *virB10*, which are unable to replicate and consequently are completely eliminated by J774 cells (Delrue *et al*., 2001). This finding supports the notion that in *Brucella* a tight transcriptional regulation of the *virB* operon is necessary to efficiently overcome the bactericidal mechanisms of the host cell.

Intracellular *virB* expression studies carried out with transcriptional fusions to P_{virB} fragments of different length revealed that the promoter and its regulatory sequences span 430 bp upstream of the transcription start site. Comparison of the intracellular and extracellular behaviour of these constructions indicated that the mechanisms that control *virB* expression within the host cell are different from those acting during vegetative growth.

We demonstrated that binding of IHF modifies the structure of the promoter inducing a DNA bending of 50.36°, indicating that IHF acts as an architectural element. In *E. coli*, IHF is involved in control of transcription of over 100 genes of widely varying function including virulence (Rowe *et al*., 2000; McLeod and Johnson, 2001). In *B. abortus*, it was suggested a role for IHF in transcriptional regulation of erythritol genes (Sangari *et al*., 2000). IHF can act as a transcriptional regulator by different mechanisms. In several cases, IHF produces a DNA bending that enables the direct interaction of a distant DNA-bound transcriptional regulator with RNA polymerase enhancing transcription (Engelhorn and Geiselmann, 1998). The second mechanism by which IHF can regulate transcription is by introducing a DNA bend that stimulates the recruitment of RNA polymerase favouring the interaction of its α-CTD domain with upstream DNA UP elements (Bertoni *et al*., 1998). In the third mechanism, the interaction of IHF with its binding site lowers the activation energy for the open complex formation (Parekh and Hatfield, 1996). In the best known examples, as those listed above, IHF is thought to act as an architectural factor that leads the correct promoter structure necessary for transcriptional regulation.

Our results suggest that *virB* operon is under complex regulatory mechanisms in which both activation and repression events could be acting. There are many examples of bacterial transcriptional regulation in which IHF (or other nucleoid proteins) acts in concert with different transcriptional regulators to repress or activate transcription (McLeod and Johnson, 2001). This is the case for the *nifA* promoter of *Herbaspirillum serpedicae*, in which IHF exerts different roles enhancing the action of NTRC and diminishing activation by NifA (Wassem *et al*., 2000). In *B. melitensis*, it was shown that an acyl-homoserine lactone is involved in P_{virB} regulation (Taminiau *et al*., 2002), suggesting that a quorum-sensing system could be one of the systems that regulates expression of *Brucella virB* operon.

The findings presented in this work constitute an approach to understand the significance of *Brucella virB* operon regulation during the infective process. Further experiments will be required to identify the environmental stimuli and regulatory mechanisms that affect the expression of this T4SS.

Experimental procedures

Media and growth conditions

Bacteria were cultured in TSB or minimal medium (Rouot *et al*., 2003) at pH 7.0 or 4.5 on a rotary shaker (250 r.p.m.) at 37°C. Media were supplemented with carbenicillin (50 μg ml^{-1}) as needed.

Plasmids

*Construction of plasmid P_{virB}::*lacZ *transcriptional fusion.* In order to amplify a 453 bp region upstream of *virB1* gene, a polymerase chain reaction (PCR) was carried out using primers pvirup (5′-GCGGATCCATGACAGGCATATTTCAAC-3′) and pvirdown (5′-ATGAATTCGATCGTCTCTTCTCAGA-3′). The PCR product was cloned into pGEM-T (Promega), generating the plasmid pGEM-T-P_{virB}. A 0.45 kb *Eco*RI fragment was excised from pGEM-T-P_{virB} and ligated to the *Eco*RI site of a *Sph*I/*Kpn*I derivative of the Amp^r plasmid pBBR1MCS-4 (Kovach *et al*., 1995), generating the plasmid pBBR-P_{virB}. Plasmid pAB2001 (Becker *et al*., 1995) was digested with *Hin*dIII (New England Biolabs), producing a 4.5 kb fragment containing a *lacZ* promoter-probe cassette. This DNA fragment was cloned into *Hin*dIII site of pBBR-P_{virB} or pBBR plasmids, generating the plasmid P_{virB}::*lacZ* transcriptional fusion (p5) and control plasmid pBBR-*lacZ* (p0).

Construction of lacZ fusions to different fragments of native P_{virB}. PCRs were carried out using forward primers pvirup, pvu77 (5′-CGGGATCCGATGCCGCCTAATGGAGC-3′), pvu144 (5′-CGGGATCCGATTCTTGGTCGGGTTAC-3′),

pvu231 (5′-CGGGATCCATACCACTTGTATATAAG-3′) or pvu300 (5′-CGGGATCCTTCTGACTGGGCGTCATTC-3′), and reverse primer pvd468 (5′-CGGGATCCGAATGGCAC CATAGGATCG-3′); and B. abortus 2308 genomic DNA was used as template. PCR products were digested with BamHI and cloned into pBBR-lacZ plasmid, generating plasmids p4, p3, p2 or p1, containing lacZ transcriptional fusions to P_{virB} fragments corresponding to positions −353 to +38, −286 to +38, −199 to +38 or −130 to +38 respectively.

The above-mentioned plasmids were introduced into wild-type *B. abortus* 2308 by electroporation.

Construction of the B. abortus *IHF expression vector.* PCRs were carried out using *B. abortus* 2308 genomic DNA as template and primers IHFACOM (5′-CTGTAAGAAGGAGAG TATCGATGGGAGGTAAAACGGTCAC-3′) and IHFAXho (5′-CCGCTCGAGCTTCGGGTTTTACCCTGAC-3′), or primers IHFBCOM (5′-CGATACTCTCCTTCTTACAGTCAGACTGCG CCGTTGAGAC-3′) and IHFBNde (5′-GGAATTCCATATG AAACAGGGGTCTAAAGCC-3′). The two PCR products, corresponding to α-*ihf* and β-*ihf* genes, were annealed and subjected to three rounds of elongation using *Pfx* (Invitrogen) and dNTPs. The elongation product was subsequently used as template in a PCR carried out with primers IHFBNde and IHFAXho. The PCR product was digested with *Nde*I and *Xho*I, and subsequently cloned into pET26b(+) expression vector (Novagen), generating the plasmid pET-*ihf*βα containing a Histidine-tagged α-*ihf* gene cloned downstream of β-*ihf* separated by a 17 bp sequence that contains a Shine-Dalgarno sequence.

Construction of plasmid pBluescript-P_{virB}*::*lacZ*.* A 0.45 kb *Eco*RI fragment was excised from pGEM-T-P_{virB} and ligated to the *Eco*RI site of plasmid pBluescript II KS (+/–) (Stratagene), generating the plasmid pBluescript-P_{virB}. Plasmid pAB2001 (Becker *et al.*, 1995) was digested with *Hin*dIII (New England Biolabs), producing a 4.5 kb DNA fragment containing a *lacZ* promoter-probe cassette. This DNA fragment was cloned into pBluescript-P_{virB}, generating the plasmid pBluescript-P_{virB}::*lacZ*.

Construction of plasmid pBluescript-$P_{virB\text{-}IHF}$-sacB/R. A 2.6 kb *Pst*I fragment was excised from plasmid pUM24 (Ried and Collmer, 1987) and ligated to *Pst*I site of plasmid pBluescript II KS (+/–), generating plasmid pBluescript-*sacB/R*. Two PCRs were carried out using *B. abortus* 2308 genomic DNA as template and primers pvirup and cIHF1COM-UP (5′-CCTGTCGAGTTGGCACCTGGCACAAAATCTTATA TACAAGT-GGT-3′), or primers pvirdownB (5′-CGGGATC CGATCGTCTCCTTCTCAGAG-3′) and cIHF1COM-DO (5′-GCCAGGTGCCAACTCGACAGGGACCAATACAAGTGCCC CA-3′). The PCR products, corresponding to two P_{virB} fragments, were annealed and subjected to three rounds of elongation using *Pfx* and dNTPs. The elongation product was subsequently used as template in a PCR carried out with primers pvirup and pvirdownB. The PCR product containing P_{virB} with a replacement of the IHF binding site was digested with *Bam*HI and cloned into plasmid pBluescript-*sacB/R*, generating plasmid pBluescript-$P_{virB\text{-}IHF}$-*sacB/R*.

Strains

Wild-type *B. abortus* 2308 strain (laboratory stock).

Construction of B. abortus *H1 mutant.* Plasmid pBluescript-$P_{virB\text{-}IHF}$-*sacB/R* was electroporated into *B. abortus* 2308. Carbenicillin^r colonies were selected as single-homologous recombinants. Single colonies were cultured overnight in rich medium (TSB) without antibiotics and plated on TSB agar containing 10% sucrose, in order to select bacteria in which plasmid pBluescript-$P_{virB\text{-}IHF}$-*sacB/R* was excised by single-homologous recombination. Single colonies were plated on TSB agar or TSB agar supplemented with carbenicillin. PCR analysis of carbenicillin^s colonies was performed with primers scrIHF1mut (whose 3′ end matches into the 20 bp sequence that replaces the IHF binding site) (5′-TATAAGATTTTGTGC CAGGT-3′) and pvirdownII. Replacement of IHF binding site sequence in positive colonies was confirmed by sequencing a 512 bp PCR product obtained with primers pvirup and pvirdownII.

Construction of B. abortus P_{virB}::lacZ *strain.* Plasmid pBluescript-P_{virB}::*lacZ* was electroporated into *B. abortus* 2308. Carbenicillin^r colonies were selected as single-homologous recombinants. Integrity of P_{virB} upstream of *lacZ* gene or upstream of the *virB* operon was confirmed by sequencing DNA fragments obtained by PCR with primers pvirup and lacZ61-43 (5′-CAGGGTTTTCCCAGTCACG-3′) or pvirup and pvirdownII.

Construction of B. abortus $P_{virB\text{-}IHF}$::lacZ *strain.* Plasmid pBluescript-P_{virB}::*lacZ* was electroporated into *B. abortus* H1. Carbenicillin^r colonies were selected as single-homologous recombinants. PCR analysis of carbenicillin^r colonies was performed with primers scrIHF1mut and lacZ61-43, or scrIHF1wt (5′-ATATAAGATTTTGTTAAAAAAGA-3′) (whose 3′ end matches into the 20 bp sequence of the native IHF binding site) and pvirdownII. Replacement of IHF binding site sequence in the promoter located upstream of *lacZ* gene was confirmed by sequencing a PCR product obtained with primers pvirup and lacZ61-43. Integrity of P_{virB} upstream of the *virB* operon was confirmed by sequencing DNA fragments obtained by PCR with primers pvirup and pvirdownII.

Cell infection assays

Murine macrophage-like J774 cells were maintained in RPMI 1640 (Gibco) supplemented with 10% fetal bovine serum and 2 mM L-glutamine. Cells seeded in 24-well plates (5×10^5 cells per well) were inoculated with 1 ml of cell culture medium (RPMI 1640 supplemented with 5% fetal bovine serum and 2 mM L-glutamine without antibiotics) containing bacteria at a multiplicity of infection of 100 (for intracellular expression experiments) or 50 (for intracellular replication assays). Multiwell plates were centrifuged for 10 min at 141 *g* at room temperature and placed in a 5% CO_2 atmosphere at 37°C. After 30 min, cells were washed four times with phosphate-buffered saline (PBS) (pH 7.4) and incubated with cell culture medium containing gentamicin (100 μg ml^{-1}) and streptomycin (50 μg ml^{-1}) to eliminate extracellular bacteria. At different times, cells were washed four times with PBS and

treated for 10 min with 1 ml of 0.1% Triton X-100 in deonized sterile water. The number of intracellular viable bacteria was determined as cfu ml^{-1} by serial dilution and plating on tryptic soy agar supplemented with antibiotics as needed.

In vitro *β-galactosidase activity assays*

In vitro β-galactosidase assays for all *lacZ* transcriptional fusion constructs (plasmid and chromosomal) were carried out with whole cells as described by Sambrook *et al*. (1989) with the following modification: reaction mixture was centrifuged before the determination of A_{420}. β-Galactosidase activity was expressed as A_{420}/volume × A_{600}.

β-Galactosidase activity assays in different media were performed as follows: bacteria were cultured in TSB, harvested during the exponential phase of growth (OD_{600} = 0.5–1), washed with PBS and resuspended in different media. β-Galactosidase activity was measured at different times.

Intracellular β-galactosidase activity assays

Murine macrophage-like J774 cells were infected with indicated strains as described. At different times p.i., cells were washed four times with PBS and treated for 10 min with 1 ml of 0.1% Triton X-100 in deonized sterile water. Two hundred microlitres of each sample were used to determine the number of intracellular viable bacteria as cfu ml^{-1} by serial dilution and plating on TSB supplemented with carbenicillin (50 μg ml^{-1}). The remaining 800 μl were used to measure β-galactosidase activity.

In experiments performed with plasmid transcriptional fusions, β-galactosidase activity was measured using a method based on that described by Sambrook *et al*. (1989) with the following modifications: in order to avoid contamination with β-galactosidase from degraded bacteria, cell lysates were centrifuged and the supernatant was discarded. Bacterial pellet was resuspended in Z buffer (60 mM Na_2HPO_4, 45 mM NaH_2PO_4, 10 mM KCl, 1.6 mM $MgSO_4 \cdot 7\ H_2O$, 35 mM β-Mercaptoethanol) (pH 7.0) and after addition of SDS, $CHCl_3$ and ONPG as described, reactions were incubated for 60 min at 28°C. Reactions were stopped with Na_2CO_3, centrifuged and A_{420} of supernatants was determined. Linearity of A_{420} along the whole incubation time was verified. Intracellular β-galactosidase activity was expressed as $A_{420} \times 10^7$/volume × cfu ml^{-1}.

In order to increase sensitivity, β-galactosidase activity of chromosomal transcriptional fusions was measured as follows: cell lysates were centrifuged and the supernatants were discarded. The bacterial pellet was resuspended in M buffer [25 mM Tris-HCl (pH 7.5), 125 mM NaCl, 2 mM $MgCl_2$, 0.3 mM 4-methylumbelliferyl-β-D-galactoside (Sigma)] and after addition of SDS and $CHCl_3$ reactions were incubated for 60 min at 37°C. Reactions were stopped by adding, after centrifugation, 100 μl of supernatant to 1.9 ml of stop buffer [133 mM Glycine, 83 mM Na_2CO_3 (pH 10.7)]. Fluorescence of samples was analysed in an AMINCO-Bowman Series 2 Luminescence Spectrometer by excitation at 365 nm and emission at 460 nm. Each measurement was calibrated with a standard curve. Intracellular β-galactosidase activity was expressed as nmol of 4-methylumbelliferone per cfu.

Primer extension analysis

Bacteria were grown in rich medium and total RNA was obtained as described by Ausubel *et al*. (1987). Primer pvirdown II (5′-GTCTGAGGTGCAACAGT-3′) was labelled with ^{32}P at the 5′ end by using [γ-^{32}P]-ATP and T4 polynucleotide kinase (New England Biolabs). For primer-RNA annealing, 20 μg of total RNA was incubated with 4×10^5 cpm of the ^{32}P-labelled primer at 70°C for 5 min, left standing at room temperature for 5 min and then put in an ice bath. Synthesis of cDNA was carried out at 42°C for 1 h using M-MLV reverse transcriptase (Gibco). Products were analysed in a 6% polyacrylamide gel in parallel with DNA sequencing reactions carried out with primer pvirdown II and visualized by autoradiography.

Gel shift experiments

The different DNA fragments for gel shift assays were produced by PCR using the following primers. The 225 bp fragment of P_{virB} (–201 to +24) was generated with primers pvirdown I (5′-GATCGTCTCCTTCTCAGAG-3′) and pvu229 (5′-CGCATACCACTTGTATATAAG-3′), and plasmid pBAuBd carrying the whole P_{virB} as template. The 226 bp fragment of *virB10* was generated with primers B10Qu (5′-CTATGCAAC CCAGAAGGTCGG-3′) and B10d (5′-GGGAATTCGTCAG GCACAATAAAGTCAC-3′), and genomic DNA of *B. abortus* 2308 as template. Probes were internally labelled through inclusion of 50 μCi [α-^{32}P]-dCTP in the PCR and subsequently purified on a native polyacrylamide gel.

Promoter fragments used as unlabelled competitors in gel shift assays were constructed by PCR using the following primers: primers pvu229 and pvirdown I for unlabelled probe –201 to +24, primers pvu300 and pvirdown I for fragment A1, primers pvu371 and pvirdown I for fragment B1 and primers pvu229 and pvd335 (5′-CGGGATCCGGGGCTATATATTGT GTGA-3′) for fragment C1, primers pvirdown I and pvu229 for the 225 bp fragment of P_{virB}, primers B10Qu and B10d for the 226 bp fragment of *virB10*.

The reactions for gel shift assays were carried out in a volume of 20 μl containing DNA-binding buffer [15 mM Tris-HCl (pH 8.0), 1 mM DTT, 0.5 mM EDTA, 10 μg ml^{-1} bovine serum albumin (BSA), 30 mM KCl, 6% glycerol, 50 μg ml^{-1} salmon sperm DNA], 10 000 cpm of the indicated ^{32}P-labelled DNA fragments, and rIHF or *B. abortus* 2308 protein extracts. After incubation at room temperature for 30 min, protein–DNA complexes were separated from the free probes by electrophoresis on 8% non-denaturing polyacrylamide gels at a constant voltage of 220 V. Gels were exposed to X-ray films and the amounts of free and protein-bound DNA were determined by measuring the intensity of the bands with a 1D 3.0 Software (Kodak). The apparent dissociation constant (K_d) was determined as the protein concentration necessary to bind 50% of the probe as described by Rhodes and Fairall (1997).

Isolation and identification of B. abortus *2308 IHF*

A bacterial pellet obtained from *B. abortus* 2308 stationary phase cultures was suspended in protoplasting buffer

[15 mM Tris-HCl (pH 7.6), 0.45 M sucrose, 8 mM EDTA] and lysozyme was added to a final concentration of 0.4 mg ml^{-1}. The suspension was incubated for 15 min at 0°C, centrifuged for 10 min at 6000 r.p.m. and resuspended in 20 mM Tris-HCl (pH 7.6), 3 mM β-Mercaptoethanol, 1 mM phenylmethysulphonyl fluoride (PMSF). This resulting suspension was disrupted by sonication (15 bursts of 30 s separated by 30 s intervals), centrifuged for 30 min at 14 000 r.p.m. and ultracentrifuged for 2.5 h at 35 500 r.p.m. The cleared lysate was subjected to an ammonium sulphate fractionation and DNA-binding activity of the different fractions was measured by gel shift assay. The positive fraction (55–75% ammonium sulphate saturation) was dialysed against buffer A [20 mM Tris-HCl (pH 7.6), 3 mM β-Mercaptoethanol] and cromatographed in a DEAE-Sepharose column. Elution was performed using buffer A with a linear gradient of NaCl (0–1 M). Sucrose was added to a final concentration of 5% to store the samples at −20°C. After DNA-binding activity analysis and dialysis, the positive pooled fractions of partially purified extract were loaded onto a Mono-Q column. Elution, DNA-binding activity analysis, dialysis and storage of the MonoQ eluates were performed as in the previous purification step.

The fourth purification step was performed as follows. A fragment of P_{virB} (positions −201 to +24) was amplified by PCR using primer pvu229, 5′-biotinilated primer pvirdown I and *B. abortus* 2308 genomic DNA as template. The biotinylated DNA was fixed to streptavidin paramagnetic spheres (Promega) and a binding reaction was performed using the MonoQ-positive pool fractions in binding buffer. After one wash with binding buffer and two washes with binding buffer without salmon sperm DNA, the DNA-bound proteins were eluted with 0.8 M NaCl. Sample was concentrated using a Centricon YM-10 (Millipore) and submitted to electrophoresis in a 15% SDS-PAGE. After Coomassie blue staining, a single band with mobility corresponding to a mass of about 12 kDa was observed. The band was cut and sent to the Proteomics Core Facility, CCFG, State University of New York at Albany (NY, USA) for sequencing by tandem mass spectrometry (MS/MS) on a LC Q-tof2 tandem mass spectrometer.

Production of recombinant IHF

Plasmid pET-*ihf*βα was introduced into *E. coli* BL21 strain and induced with isopropyl-β-D-thioglactopyranoside. Bacteria were centrifuged, resuspended in buffer B [20 mM Tris-HCl (pH 7.6), 1 mM PMSF] and disrupted by sonication. The sonic extract was centrifuged for 30 min at 14 000 r.p.m. NaCl was added to a final concentration of 0.35 M and sample was loaded into a Hi-Trap Nickel-chelating column (Amersham Biosciences). Elution was performed using buffer C [20 mM Tris-HCl (pH 7.6), 0.35 M NaCl] with a linear gradient of imidazole (0–1 M). Sucrose was added to a final concentration of 5% to store the samples at −20°C. Eluates were analysed in a 15% SDS-PAGE, and a fraction containing both subunits of rIHF with a purity of about 95% was obtained.

DNase I footprinting

The fragment of P_{virB} used in DNase I footprinting was generated as follows. The oligonucleotide primer pvirdown I was 5′ end-labelled with ^{32}P by using [γ-^{32}P]-ATP and T4 polynucleotide kinase (New England Biolabs). The DNA fragment was amplified by PCR using the ^{32}P-labelled primer pvirdown I, primer pvu229 and the plasmid pBAuBd carrying the entire P_{virB} as template. The PCR product was then purified on a native polyacrylamide gel. DNase I footprinting experiments were performed with the same binding protocol as in gel shift experiments using 1.2×10^5 cpm of the ^{32}P-labelled probe and different concentrations of rIHF. After protein binding, $MgCl_2$ and $CaCl_2$ concentrations were adjusted to 1.5 and 0.5 mM, respectively, and each reaction mixture was incubated with 1 U of RQ1 DNase I (Promega) for 1 min at room temperature. Reactions were stopped by the addition of 5 μl of stop solution (25 mM EDTA, 0.6 M sodium acetate). Digested products were extracted by phenol-chloroform, ethanol precipitated and resuspended in 4 μl of sequencing gel loading buffer. DNA fragments were then separated on a 6% polyacrylamide DNA sequencing gel and visualized by autoradiography. DNA sequencing reactions carried out with primer pvirdown I were used to localize the position of the protected regions.

AFM analysis

The fragment of P_{virB} used in AFM assays was produced by PCR using the primers pvirup and pvirdown II, *Pfx* (Invitrogen) and genomic DNA of *B. abortus* 2308 as template. PCR products were extracted by chloroform-isoamylic alcohol, ethanol precipitated and resuspended in MilliQ water previously filtered through a 0.2 mm filter (Millipore). The binding reactions were carried out in a volume of 20 μl containing DNA-binding buffer [15 mM Hepes (pH 7.9), 30 mM KCl, 6% glycerol], 20 ng of the 512 bp DNA fragment and 185 nM rIHF. After incubation at room temperature for 25 min, sample was diluted 10-fold into 15 mM Hepes (pH 7.9), 10 mM $MgCl_2$, and aliquots of 20 μl were deposited on mica. After 5 min in an humidifying chamber, the mica disc was washed with 1 ml of MilliQ water (Millipore) and dried briefly in a gentle stream of nitrogen. Tapping mode AFM was performed in dry nitrogen using a Nanoscope III Multimode-AFM (Digital Instruments-Vecco) with a J-type scanner having a maximal lateral range of 150 μm. Standard silicon cantilevers 125 μm in length were used. Cantilever oscillation frequency was tuned to the resonance frequency of the cantilever (300 kHz). 512×512 pixel images were captured with a scan size between 0.6 and 5 μm at a scan rate of one to two scan lines per second. Images were processed by flattening using NANOSCOPE software (Digital Instruments) to remove background slope. The same software was used to measure the DNA bending angles at the protein binding sites by drawing lines through the DNA axes on both sides of the protein and measuring the angle at their intersection (Rees *et al.*, 1993). The DNA bending angle is defined as $\theta = 180 - \alpha$. The mean ± SD of DNA bend angle was measured from AFM images of 40 rIHF–P_{virB} complexes.

Acknowledgements

We thank Dr C.C. Frasch for reading the manuscript and Silvio J. Ludueña and María M. Echarte for help with AFM.

We also thank Quishan Lin for help with mass spectrometry sequencing. This work was supported by Grant No. 14116-187 to L.I.P. from Fundancion Antorchas, Buenos Aires, Argentina; and Grants PICT2002 No. 01-11882 to D.J.C. and PICT2000 No. 01-09194 to R.A.U. from Agencia Nacional de Promocion Cientifica y Tecnologica, SECyT, Buenos Aires, Argentina.

References

Ausubel, F.M., Brent, R., Kingston, R.E., Moore, D.D., Seidman, J.G., Smith, J.A., *et al.* (1987) *Current Protocols in Molecular Biology*. New York: Wiley-Interscience.

Becker, A., Schmidt, M., Jager, W., and Puhler, A. (1995) New gentamicin-resistance and lacZ promoter-probe cassettes suitable for insertion mutagenesis and generation of transcriptional fusions. *Gene* **162:** 37–39.

Bertoni, G., Fujita, N., Ishihama, A., and de Lorenzo, V. (1998) Active recruitment of sigma54-RNA polymerase to the Pu promoter of *Pseudomonas putida*: role of IHF and alphaCTD. *EMBO J* **17:** 5120–5128.

Boschiroli, M.L., Ouahrani-Bettache, S., Foulongne, V., Michaux-Charachon, S., Bourg, G., Allardet-Servent, A., *et al.* (2002) The *Brucella suis virB* operon is induced intracellularly in macrophages. *Proc Natl Acad Sci USA* **99:** 1544–1549.

Bustamante, C., and Rivetti, C. (1996) Visualizing protein–nucleic acid interactions on a large scale with the Scanning Force Microscopy. *Annu Rev Biophys Biomol Struct* **25:** 395–429.

Celli, J., and Gorvel, J.P. (2004) Organelle robbery: *Brucella* interactions with the endoplasmic reticulum. *Curr Opin Microbiol* **7:** 93–97.

Celli, J., de Chastellier, C., Franchini, D.M., Pizarro-Cerda, J., Moreno, E., and Gorvel, J.P. (2003) *Brucella* evades macrophage killing via VirB-dependent sustained interactions with the endoplasmic reticulum. *J Exp Med* **198:** 545–556.

Comerci, D.J., Martinez-Lorenzo, M.J., Sieira, R., Gorvel, J.P., and Ugalde, R.A. (2001) Essential role of the VirB machinery in the maturation of the *Brucella abortus*-containing vacuole. *Cell Microbiol* **3:** 159–168.

Conover, G.M., Derre, I., Vogel, J.P., and Isberg, R.R. (2003) The *Legionella pneumophila* LidA protein: a translocated substrate of the Dot/Icm system associated with maintenance of bacterial integrity. *Mol Microbiol* **48:** 305–321.

Corbel, M.J. (1997) Brucellosis: an overview. *Emerg Infect Dis* **3:** 213–221.

Covacci, A., Telford, J.L., Del Giudice, G., Parsonnet, J., and Rappuoli, R. (1999) *Helicobacter pylori* virulence and genetic geography. *Science* **284:** 1328–1333.

Delrue, R.M., Martinez-Lorenzo, M., Lestrate, P., Danese, I., Bielarz, V., Mertens, P., *et al.* (2001) Identification of *Brucella* spp. genes involved in intracellular trafficking. *Cell Microbiol* **3:** 487–497.

Engelhorn, M., and Geiselmann, J. (1998) Maximal transcriptional activation by the IHF protein of *Escherichia coli* depends on optimal DNA bending by the activator. *Mol Microbiol* **30:** 431–441.

Hong, P.C., Tsolis, R.M., and Ficht, T.A. (2000) Identification of genes required for chronic persistence of *Brucella abortus* in mice. *Infect Immun* **68:** 4102–4107.

Kovach, M.E., Elzer, P.H., Hill, D.S., Robertson, G.T., Farris, M.A., Roop, R.M., 2nd, and Peterson, K.M. (1995) Four new derivatives of the broad-host-range cloning vector pBBR1MCS, carrying different antibiotic-resistance cassettes. *Gene* **166:** 175–176.

Lestrate, P., Delrue, R.M., Danese, I., Didembourg, C., Taminiau, B., Mertens, P., *et al.* (2000) Identification and characterization of *in vivo* attenuated mutants of *Brucella melitensis*. *Mol Microbiol* **38:** 543–551.

Li, P.L., Everhart, D.M., and Farrand, S.K. (1998) Genetic and sequence analysis of the pTiC58 trb locus, encoding a mating-pair formation system related to members of the type IV secretion family. *J Bacteriol* **180:** 6164–6172.

McLeod, S.M., and Johnson, R.C. (2001) Control of transcription by nucleoid proteins. *Curr Opin Microbiol* **4:** 152–159.

O'Callaghan, D., Cazevieille, C., Allardet-Servent, A., Boschiroli, M.L., Bourg, G., Foulongne, V., *et al.* (1999) A homologue of the *Agrobacterium tumefaciens* VirB and *Bordetella pertussis* Ptl type IV secretion systems is essential for intracellular survival of *Brucella suis*. *Mol Microbiol* **33:** 1210–1220.

Parekh, B.S., and Hatfield, G.W. (1996) Transcriptional activation by protein-induced DNA bending: evidence for a DNA structural transmission model. *Proc Natl Acad Sci USA* **93:** 1173–1177.

Pietrasanta, L.I., Thrower, D., Hsieh, W., Rao, S., Stemmann, O., Lechner, J., *et al.* (1999) Probing the *Saccharomyces cerevisiae* centromeric DNA (*CEN* DNA)-binding factor 3 (CBF3) kinetochore complex by using atomic force microscopy. *Proc Natl Acad Sci USA* **96:** 3757–3762.

Pizarro-Cerda, J., Moreno, E., Sanguedolce, V., Mege, J.L., and Gorvel, J.P. (1998) Virulent *Brucella abortus* prevents lysosome fusion and is distributed within autophagosome-like compartments. *Infect Immun* **66:** 2387–2392.

Rees, W.A., Keller, R.W., Vesenka, J.P., Yang, G., and Bustamante, C. (1993) Evidence of DNA bending in transcription complexes imaged by scanning force microscopy. *Science* **260:** 1646–1649.

Rhodes, D., and Fairall, L. (1997) Analysis of sequence-specific DNA-binding proteins. In *Protein Function.* Creighton, T.E. (ed.). New York: Oxford University Press, pp. 215–244.

Ried, J.L., and Collmer, A. (1987) An *nptI-sacB-sacR* cartridge for constructing directed, unmarked mutations in gram-negative bacteria by marker exchange-eviction mutagenesis. *Gene* **57:** 239–246.

Rouot, B., Alvarez-Martinez, M.T., Marius, C., Menanteau, P., Guilloteau, L., Boigegrain, R.A., *et al.* (2003) Production of the type IV secretion system differs among *Brucella* species as revealed with VirB5- and VirB8-specific antisera. *Infect Immun* **71:** 1075–1082.

Rowe, S., Hodson, N., Griffiths, G., and Roberts, I.S. (2000) Regulation of the *Escherichia coli* K5 capsule gene cluster: evidence for the roles of H-NS, BipA, and integration host factor in regulation of group 2 capsule gene clusters in pathogenic *E. coli*. *J Bacteriol* **182:** 2741–2745.

Sambrook, J., Fritsch, E.F., and Maniatis, T. (1989) *Molecu-*

lar Cloning: A Laboratory Manual. Cold Spring Harbor, New York: Cold Spring Harbor Laboratory Press.

Sangari, F.J., Aguero, J., and Garcia-Lobo, J.M. (2000) The genes for erythritol catabolism are organized as an inducible operon in *Brucella abortus*. *Microbiology* **146:** 487–495.

Schmiederer, M., Arcenas, R., Widen, R., Valkov, N., and Anderson, B. (2001) Intracellular induction of the *Bartonella henselae virB* operon by human endothelial cells. *Infect Immun* **69:** 6495–6502.

Sieira, R., Comerci, D.J., Sanchez, D.O., and Ugalde, R.A. (2000) A homologue of an operon required for DNA transfer in *Agrobacterium* is required in *Brucella abortus* for virulence and intracellular multiplication. *J Bacteriol* **182:** 4849–4855.

Stachel, S.E., and Nester, E.W. (1986) The genetic and transcriptional organization of the vir region of the A6 Ti plasmid of *Agrobacterium tumefaciens*. *EMBO J* **5:** 1445–1454.

Taminiau, B., Daykin, M., Swift, S., Boschiroli, M.L., Tibor, A., Lestrate, P., *et al.* (2002) Identification of a quorum-sensing signal molecule in the facultative intracellular pathogen *Brucella melitensis*. *Infect Immun* **70:** 3004–3011.

Thompson, D.V., Melchers, L.S., Idler, K.B., Schilperoort, R.A., and Hooykaas, P.J. (1988) Analysis of the complete nucleotide sequence of the *Agrobacterium tumefaciens virB* operon. *Nucleic Acids Res* **16:** 4621–4636.

Ugalde, R.A. (1999) Intracellular lifestyle of *Brucella* spp. Common genes with other animal pathogens, plant pathogens, and endosymbionts. *Microbes Infect* **1:** 1211–1219.

Wassem, R., De Souza, E.M., Yates, M.G., Pedrosa, F.D., and Buck, M. (2000) Two roles for integration host factor at an enhancer-dependent *nifA* promoter. *Mol Microbiol* **35:** 756–764.

Weiss, A.A., Johnson, F.D., and Burns, D.L. (1993) Molecular characterization of an operon required for pertussis toxin secretion. *Proc Natl Acad Sci USA* **90:** 2970–2974.

Winans, S.C., and Walker, G.C. (1985) Conjugal transfer system of the IncN plasmid pKM101. *J Bacteriol* **161:** 402–410.